Molecular Self-Diffusion in Micellar and Discrete Cubic Phases of an Ionic Surfactant with Mixed Monovalent/Polymeric Counterions

Anna Svensson, Daniel Topgaard, Lennart Piculell,* and Olle Söderman

Physical Chemistry 1, Center for Chemistry and Chemical Engineering, Lund University, P.O. Box 124, S-221 00 Lund, Sweden

Received: March 31, 2003; In Final Form: August 28, 2003

The molecular self-diffusion in concentrated aqueous mixtures based on an oppositely charged polymer−surfactant pair has been investigated by NMR pulsed field gradient techniques. The investigated structures were an ordered cubic *Pm*3*n* phase (ca. 50 wt % water) and a disordered micellar phase, both containing cetyltrimethylammonium (CTA^+) micelles with mixed acetate (Ac^-) and polyacrylate (PA^-) counterions. In the cubic phase, CTA^+ gave broad lines in the ^1H NMR spectrum, which made it possible to use the pulsed field gradient (PFG) spin echo (SE) technique to measure the PA^- diffusion. The observed diffusion coefficients for the four different molecular species covered 4 orders of magnitude with the rate of diffusion decreasing in the order water > Ac^- > PA^- > CTA^+. For all species, the diffusion coefficients were largely insensitive to the counterion composition. A model considering obstruction effects and binding to the micelles could account for the reduced diffusion of Ac^- and CTA^+ compared to dilute reference solutions. For water, the reduction of the diffusion was mainly due to obstruction effects. The PA^- diffusion was much more retarded than the Ac^- diffusion in the cubic phase; moreover, the molecular weight dependence of the diffusion was dramatically enhanced for the polydisperse polyion. Both effects are attributed to electrostatic attractions and obstruction effects experienced by polyions diffusing in a concentrated matrix of stationary micelles.

Introduction

Oppositely charged polymers and surfactants exhibit a rich and interesting behavior in water, as demonstrated by a considerable research effort over the past decades.[1,2] An associative phase separation often occurs, resulting in one concentrated phase (a precipitate or a coacervate) rich in polyions and surfactant ions and one dilute phase containing most of the simple counterions.[3−5] In recent years, focus has turned to the compositions and structures of the various concentrated phases.[6−11] The concentrated phase sometimes contains highly ordered structures made up by surfactant aggregates with polyions as counterions.

We recently introduced a new approach to the study of oppositely charged polymer−surfactant mixtures.[12] The essence of this approach is to use the minimum number of components when varying the ratio of polyions to surfactant ions in the mixtures. To that end, we first synthesize the pure *polyion−surfactant ion complex salt* and use this as our point of departure. By mixing the complex salt with the conventional surfactant (surfactant ion + simple counterion) in water, we obtain a truly ternary system containing surfactant aggregates with mixed polyions/simple ions as counterions (see Figure 1). The fraction of polyions can obviously be varied from zero to unity. It is important to realize that this system contains no excess salt but only the counterions (polyions and simple ions) neutralizing the surfactant aggregates.

Using the above approach, we recently encountered a particularly simple phase diagram, see Figure 2.[13] The studied complex salt was cetyltrimethylammonium polyacrylate (CTA-PA), which contains a short polyacrylate as the polymeric counterion, and the surfactant was cetyltrimethylammonium acetate (CTAAc). Acetate contains the same charged group, the carboxylate group, as polyacrylate. Therefore, mixtures of CTAPA and CTAAc illustrate mixtures with monomeric and polymeric counterions of close chemical similarity. Moreover, the attraction between the surfactant aggregates and the counterions is essentially only electrostatic.[8]

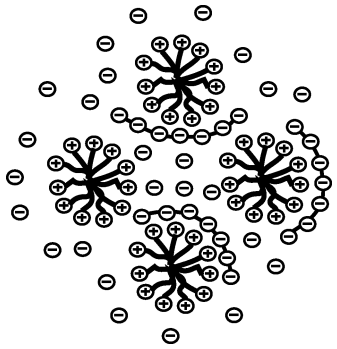

Figure 1. Mixing the complex salt, surfactant, and water gives a truly ternary system, which contains surfactant aggregates with oppositely charged polymeric or monovalent counterions. See text for details.

One striking feature of the CTAPA/CTAAc/water phase diagram (Figure 2) is that the shapes of the surfactant aggregates are insensitive to the ratio of polymeric/monomeric counterions. At the lowest investigated water contents, a hexagonal phase of cylindrical surfactant aggregates is formed, irrespective of the counterion composition. At all higher water contents, from around ca. 50 wt % and above, the aggregates are always small micelles. In essence, the latter part of the phase diagram describes an aqueous system of nearly spherical colloidal particles (the surfactant micelles) with mixed monomeric/polymeric counterions. At high concentrations, the micelles

* Corresponding author. E-mail: lennart.piculell@fkem1.lu.se. Tel: +46-46-222 95 18. Fax: +46-46-222 44 13.

10.1021/jp0348225 CCC: $25.00
Published on Web 11/01/2003

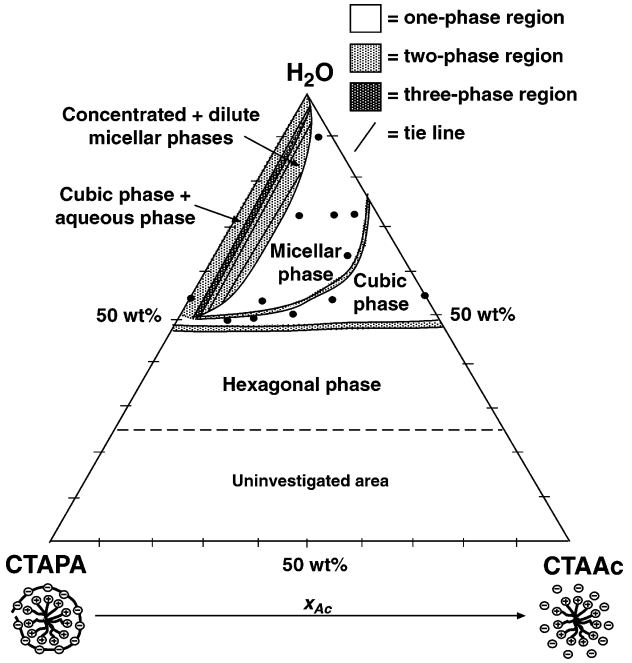

Figure 2. Experimental phase diagram of the complex salt CTAPA, the surfactant CTAAc, and water at 25 °C.[13] Points denote compositions of the samples studied in the present investigation.

crystallize into a cubic phase with a *Pm*3*n* structure. The cubic phase extends across the entire phase diagram from the binary CTAPA/water axis to the binary CTAAc/water axis. For pure CTAPA in water, the cubic phase region is quite narrow; its maximum water uptake is ca. 55 wt % water. Samples containing more water are biphasic with a cubic phase in equilibrium with essentially pure water. This phase behavior is a manifestation of the strong bridging attraction that operates between micelles neutralized by only polymeric counterions.[8] The surfactant CTAAc, on the other hand, is completely miscible with water. Its cubic phase can absorb large quantities of water (75 wt %) before it "melts" into a disordered micellar phase. The large extension of the cubic phase of CTAAc is due to the long-range double-layer repulsion between micelles neutralized by only monovalent counterions. Mixtures of CTAPA and CTAAc, finally, display a transition between the soluble CTAAc micelles and the insoluble CTAPA micelles. One of the features of these mixtures is a large micellar phase, which extends to quite high contents of polymeric counterions, especially for concentrated mixtures.

To the best of our knowledge, there are no previous studies of molecular diffusion in concentrated phases of oppositely charged surfactants and polymers. The simple composition and the simple phase behavior of the CTAPA/CTAAc/water mixtures make the system extremely well suited for such investigations. More specifically, it offers a possibility to study how the diffusion coefficients of the various molecular species in a single phase (the cubic phase) are affected by varying, over the entire range, the proportions of monomeric and polymeric counterions. Moreover, it is possible to study the effects of a structural change, from an ordered cubic to a disordered micellar phase, that involves very small changes in the size and shape of the surfactant aggregates. From another perspective, the cubic phase offers a well-defined structure for studies of polymer diffusion in a concentrated structured medium, which is of fundamental interest.[14]

The aim of the present study is to investigate the molecular self-diffusion of water, surfactant, and polymeric and monovalent counterions in the cubic and micellar phases of the CTAPA/CTAAc/water system. To this end, we use the NMR self-diffusion technique. This is a versatile technique for the study of structure and dynamics in surfactant and polymer systems.[15] The method monitors molecular displacements on the millisecond time scale and the micrometer length scale. It thus provides average molecular diffusion coefficients in self-assembled surfactant systems that are homogeneous on that length scale. With the NMR method, it is in principle possible to measure, within a few minutes, the self-diffusion of all proton-containing components in a mixture.

Materials and Methods

Materials. Poly(acrylic acid) (HPA) 2000 g/mol was purchased from Aldrich. The same product, but not the same batch, has been examined in previous studies by size-exclusion chromatography coupled with low-angle light scattering, giving a number-average molar mass, M_n, of 2800 g/mol and a weight-average mass, M_w, of 4700 g/mol.[5] The number-average degree of polymerization is approximately 30, giving a length of 7.5 nm for a fully extended chain.

The HPA was purified by dialysis for 5 days against Millipore water, followed by freeze-drying. ^{1}H NMR revealed a small amount of a structural impurity in the polymer, which remained at unchanged intensity even after the dialysis procedure. Two different batches of HPA both showed the presence of the impurity, which we tentatively ascribe to heterounits at the ends of the short polymer, originating from a termination reaction in the synthesis procedure. Titration of HPA with NaOH showed that the equivalent molar mass of the HPA was 89.3 g/(mole of carboxylic acid), as compared to the theoretical value of 72 g/mol for a repeating unit of HPA. Presumably, this difference is due primarily to the heterounits in the polymer. The contribution from water to the equivalent molar mass should be small. The water uptake of freeze-dried HPA exposed to ambient air was found to be 2 wt % after 1 h and 5 wt % after several days.

Cetyltrimethylammonium bromide, CTABr, was purchased from Merck and used without further purification. The molar mass of CTABr is 364.5 g/mol.

The complex salt, CTAPA, was prepared by titrating the hydroxide form of the surfactant with HPA. The first step was to convert CTABr into CTAOH by ion exchange.[16] The ion-exchange resin (Dowex SBR, dry mesh 20−50, from Sigma) was charged by stirring in excess amount of 1 M NaOH for 2 h and then rinsed with Millipore water until the rinsing water reached pH 7. CTABr (30 g) was then dissolved in a plastic beaker containing a large excess (200 g) of the charged ion-exchange resin and 250 mL of Millipore water. The solution was stirred until all CTABr was dissolved. The slurry was filtered, and the filtrate was rinsed with Millipore water into a fresh batch of 200 g of resin and 250 mL of water, and the mixture was stirred for another 2 h. The last step was repeated once. The alkaline solution now contained CTAOH at a concentration of approximately 0.05 M. A 0.5 M solution of HPA was titrated dropwise into the freshly prepared solution of CTAOH under stirring. This was done immediately to avoid Hofmann elimination of the quaternary ammonium hydroxide group of the surfactant in the basic solution.[17] The pH was measured using a standard pH electrode. A white precipitate, the complex salt, was formed at the start of the titration, which was continued until the equivalence point was reached in the solution. The latter point was taken as the inflection point (pH = 8.6) in the pH titration curve, determined in a separate

measurement. After equilibration overnight, the solution with the precipitate was freeze-dried. The complex salt was then obtained as a white, hygroscopic powder, which was then stored over silica gel in a desiccator. Titrimetric analysis gave a bromide content below the detection limit (0.3 wt %) in the complexes.

The surfactant cetyltrimethylammonium acetate (CTAAc) was prepared by the same procedure, that is, by titrating CTAOH with acetic acid, HAc, to the equivalence point (pH 8.1). The resulting CTAAc solution was clear. After freeze-drying, CTAAc was obtained as a white powder and stored over a silica gel in a desiccator.

Sodium polyacrylate, NaPA, was prepared by titrating the poly(acrylic acid) with sodium hydroxide to the equivalence point (pH 8.6), followed by freeze-drying and storage in desiccator. The simple salt sodium acetate, NaAc (AnalaR, BDH, England) was dried in an oven and stored in a desiccator.

Weighing experiments indicated water contents of CTAPA and CTAAc of approximately 10 wt % over silica gel in the desiccator and 20 wt % after prolonged storage in air. The water content of the polyelectrolyte NaPA was also 10 wt % in the desiccator but approximately 50 wt % after prolonged storage in air. Care was taken to minimize the exposure of the components to air during sample preparation. A water content of 10 wt % in CTAPA, CTAAc, NaPA, and NaAc was assumed when calculating the sample compositions.

The fraction of acetate vs polyacrylate counterions in a sample in the phase diagram will be expressed in terms of equivalent charge as

$$x_{Ac} = \frac{n_{Ac}}{(n_{Ac} + n_{PA})} \quad (1)$$

where n_i refers to the total number of charges from species i in the mixture. Thus, $x_{Ac} = 0$ refers to a sample containing only polyacrylate counterions, whereas $x_{Ac} = 1$ means a sample with only acetate counterions.

Sample Preparation. Two sets of samples for the SAXS and NMR experiments were prepared with identical molar compositions but with normal water for the SAXS experiments and deuterated water for the samples studied by NMR. Sample compositions, given in weight percent throughout, refer to the mixtures prepared in normal water.

Samples used for SAXS measurements were prepared as follows. Appropriate amounts of complex salt, surfactant, and water were weighed and put in glass tubes. After the samples were mixed with a Vortex vibrator, the tubes were flame-sealed. The mixing was continued in a centrifuge at 4000 rpm and 40 °C with a rotor of the radius 15 cm during 6 h. The tubes were turned end-over-end every 15 min. The samples were left to equilibrate at 25 °C for several weeks.

Samples used for NMR studies were prepared by mixing appropriate amounts of complex salt, surfactant, and deuterated water (D_2O). Cubic samples were centrifuged and equilibrated as described above. A piece of the cubic phase was punched out with a glass pipe and put into a 5 mm (o.d.) NMR glass tube. For the disordered micellar samples, the components were weighed directly into the NMR glass tubes, followed by mixing with a Vortex vibrator and centrifugation at 2000 rpm.

Structures and Compositions of Equilibrium Phases. All samples were investigated by visual inspection in normal light and between crossed polarizers to ensure that they were optically isotropic. This is a sensitive test for possible contamination by the hexagonal phase, which is strongly birefringent. SAXS measurements were performed with two different setups. At the D 43 instrument at L.U.R.E. in Orsay, France, a parallel monochromatic beam of wavelength 1.445 Å was focused with point collimation on the sample. The sample was contained in a flat cell with mica windows kept at 25 °C. The sample-to-detector distance was 377 mm. A Kratky compact small-angle system with linear collimation was used at the Lund laboratory. The X-rays were detected with a position-sensitive detector. The wavelength was 1.54 Å, and the sample-to-detector distance was 277 mm. The sample cell had mica windows and was maintained at 25 °C.

NMR Self-Diffusion Measurements and Data Analysis. The NMR method used to measure self-diffusion coefficients, D, relies on the application of two pulsed field gradients (PFGs) in the dephasing and refocusing periods of a spin−echo (SE), $90°-\tau-180°-\tau-$echo, or a stimulated echo (STE), $90°-\tau_1-90°-\tau_2-90°-\tau_1-$echo, pulse sequence. A detailed description of the methods can be found elsewhere.[18,19] The intensity, I, of the echo is given by

$$I = I_0 \exp(-2\tau/T_2) \exp[-\gamma^2 g^2 \delta^2 (\Delta - \delta/3) D] \quad (2)$$

for the PFG SE and

$$I = \frac{I_0}{2} \exp(-2\tau_1/T_2 - \tau_2/T_1) \exp[-\gamma^2 g^2 \delta^2 (\Delta - \delta/3) D] \quad (3)$$

for the PFG STE technique. In eqs 2 and 3, I_0 is the intensity of the signal following a single 90° pulse, γ is the magnetogyric ratio of the studied nucleus, T_1 and T_2 are the longitudinal and transverse relaxation times, respectively, and Δ is the separation between the leading edges of the PFGs with duration δ and strength g. The experiment is performed by acquiring the signal for a series of values of g. For data evalution purposes, eqs 2 and 3 can be rewritten as

$$E(k) = \exp(-kD) \quad (4)$$

where $E(k)$ is the echo attenuation normalized to zero gradient strength and $k = \gamma^2 g^2 \delta^2 (\Delta - \delta/3)$.

The signal from a multicomponent system is a superposition of the signals from the different components. The signals can be resolved with respect to chemical shift, relaxation times, and self-diffusion. The PFG SE method is used for species with fast diffusion and long T_2, while the PFG STE technique is applied to components with short T_2, long T_1, and slow diffusion.

The NMR measurements were performed on a Bruker DMX 200 spectrometer operating at 200.13 MHz proton resonance frequency. Pulsed field gradients (PFGs) were generated in a Bruker DIFF-25 gradient probe driven by a BAFPA-40 unit.

The self-diffusion of water and acetate was followed with the PFG SE pulse sequence using the parameters $\delta = 0.5$ ms, $\Delta = 20.7$ ms, and maximum $g = 9.63$ T/m. PA diffusion was measured with the same sequence but with the parameters $\delta = 3$ ms, $\Delta = 23.2$ ms, and maximum $g = 9.63$ T/m. CTA diffusion was measured with the PFG STE technique using $\delta = 1$ ms, $\Delta = 1000$ ms, and maximum $g = 9.63$ T/m.

The diffusion coefficients D_{HDO}, D_{Ac}, and D_{CTA} for water, acetate, and the surfactant ion, respectively, were obtained by regressing eq 4 onto the experimental data. With the exception of the diffusion coefficient of CTA, the errors in the obtained diffusion coefficients are typically 5% or better, as judged from the regression analyses of the raw data. Because D_{CTA} for the cubic phase is close to the lower limit of what can be measured with the equipment used here, these values should be taken as

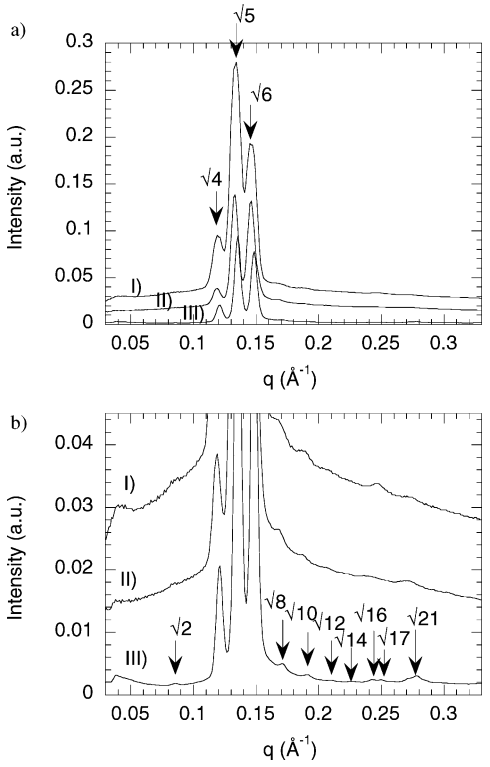

Figure 3. SAXS spectra (a) of three cubic *Pm*3*n* samples at 25 °C, (I) $x_{Ac} = 1$ at 55 wt % water (pure CTAAc), (II) $x_{Ac} = 0.3$ at 51 wt % water, and (III) $x_{Ac} = 0$ at 55 wt % water (pure CTAPA) and an enlargement (b) of the spectra, showing the relative positions of the small peaks. The relative positions of the peaks are indicated.

TABLE 1: Investigated Samples in the Cubic Phase[a]

x_{Ac}	water content (wt %)	unit cell (Å)	ϕ_{surf}[b]	N_{agg}[c]
1	55.4	104.2	0.37	110
0.6	54.9	106.0	0.36	113
0.45	52.1	105.3	0.38	116
0.3	50.9	105.6	0.38	120
0.2	50.3	103.9	0.38	113
0	54.6	103.4	0.35	100

[a] The sample compositions are indicated in the phase diagram in Figure 2. [b] Volume fraction of surfactant chains, ϕ_{surf}, calculated from the weight fraction of CTA^+, assuming a density of 1 g/cm^3. [c] Calculated as the number concentration of surfactant ions (obtained assuming a density of 1 g/cm^3 for the samples) divided by the number concentration of micelles (obtained from the unit cell dimensions with eight micelles per unit cell).

order of magnitude estimates. The evaluation of the PA^- diffusion, which is complicated by polydispersity effects, will be described in detail below.

Results

Investigated Samples and Their Characterization. The compositions of the investigated samples are indicated by points in the phase diagram in Figure 2. The cubic samples were mixed at an approximately constant content of water (50−55 wt %) with different fractions of acetate counterions, see Table 1.

The Cubic Phase. Cubic samples are transparent, stiff, and optically isotropic. SAXS diagrams from three cubic samples ($x_{Ac} = 0$, 0.3, and 1) are shown in Figure 3. The structure is of the *Pm*3*n* type and contains discrete micellar aggregates packed in a cubic array. The organization of the cubic *Pm*3*n* structure has been highly debated, but the present opinion is that it

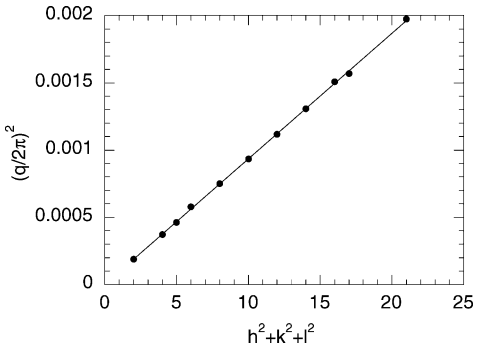

Figure 4. A plot of $(q/2\pi)^2$ vs the Miller indices of the *Pm*3*n* unit cell, according to eq 5. The q values refer to the peak positions from spectrum III in Figure 3b. The fit gives 103.4 Å for the size of the cubic unit cell.

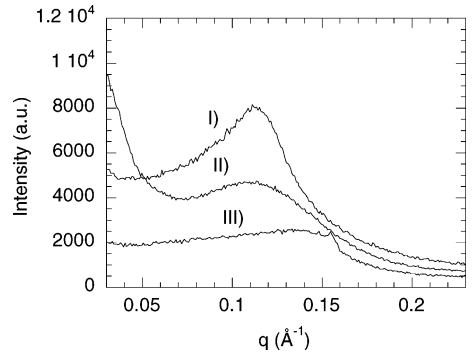

Figure 5. SAXS spectra of three micellar samples at 73 wt % water and 25 °C: (I) $x_{Ac} = 0.85$; (II) $x_{Ac} = 0.7$; (III) $x_{Ac} = 0.45$.

contains a body-centered cubic lattice with eight slightly aspherical micelles, which are placed in the center, at the corners, and in the walls of the lattice cell.[20] The structure gives rise to diffraction patterns in X-ray measurements, with peaks at the relative positions √2, √4, √5, √6, √8, √10, √12, √13, √14, √16, √17, √18, √20, √21, etc. The relative positions of the peaks are indicated in Figure 3.

The size of the unit cell, a, was obtained by plotting $(q/(2\pi))^2$ vs the Miller index of the *Pm*3*n* unit cell according to

$$\left(\frac{q}{2\pi}\right)^2 = \left(\frac{1}{a}\right)^2 (h^2 + k^2 + l^2) \qquad (5)$$

Figure 4 shows a fit of the peak positions from the cubic SAXS spectrum at $x_{Ac} = 0$ (spectrum III in Figure 3), giving a *Pm*3*n* unit cell size of 103.4 Å. The dimension of the unit cell is hardly affected by changes in the counterion composition, see Table 1. Micellar aggregation numbers were calculated assuming a density of 1 g/cm^3 for all samples, see Table 1. The mean aggregation number is only 18% larger than the theoretical value $N_{agg} = 95$ for a spherical micelle made up of cetyl surfactants with a radius corresponding to the length of a C_{16} chain.[21] This confirms that the micelles deviate only slightly from the spherical shape.

The Micellar Phase. Micellar samples are transparent and fluid. The viscosity increases with an increasing overall concentration or with an increasing fraction of polymeric counterions. SAXS diagrams of samples with changing x_{Ac} at a constant water content of 73 wt % are shown in Figure 5. The position of the maximum of the broad micellar peak corresponds to the distance between the center of the micelles as $q = 2\pi/d$. Polyacrylate counterions introduce attractive bridging interactions between neighboring micelles.[13] This leads to a clustering of the micelles and a larger distribution of the

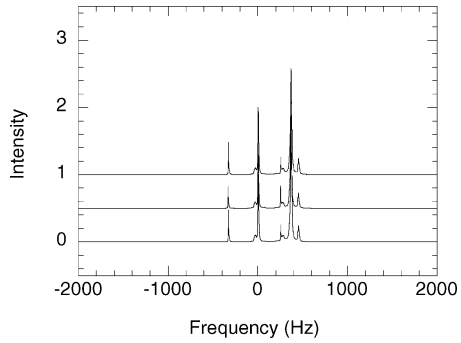

Figure 6. ^{1}H NMR spectra of the micellar phase at 73 wt % water: from top to bottom, $x_{Ac} = 0.85$, 0.7, and 0.45.

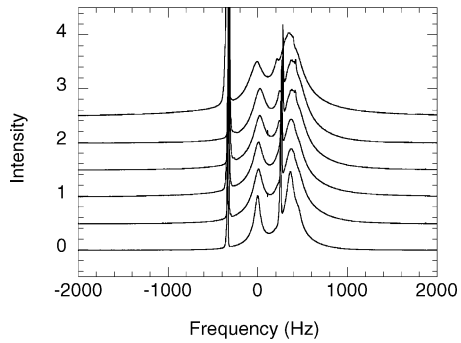

Figure 7. ^{1}H NMR spectra of the cubic phase: from top to bottom, $x_{Ac} = 1$, 0.6, 0.45, 0.3, 0.2, and 0.

characteristic distances in the sample. The clustering becomes more important with an increasing polyacrylate content. This is seen as a broadening of the micellar peak in the SAXS diagrams of Figure 5.

The disordered micellar phase extends to quite concentrated samples at high fractions of polymeric counterions. The micellar samples can still be poured at water contents as low as 52 wt %.

NMR Spectra. ^{1}H NMR spectra from disordered micellar and cubic samples are displayed in Figures 6 and 7, respectively. Both spectra are dominated by the numerous methylene protons of the CTA^+ ions. It is a striking observation that micellar solutions give narrow CTA^+ peaks, while the peaks from the cubic phase are broad. This is a consequence of the change in the aggregate dynamics as one enters the cubic phase. The micellar size is similar in the two phases (see above) in agreement with findings from analogous systems.[22] In NMR, the line width of a particular peak is given by the spin−spin relaxation time, T_2. For the present situation, a change in this quantity is determined by the molecular dynamics, which modulates the (residual) dipolar spin−spin coupling. In the micellar phase, the surfactant dynamics is given by the micellar rotational diffusion and the lateral diffusion of the surfactant over the curved micellar surface. These are relatively rapid processes, and hence, the surfactant peaks are relatively narrow.[23] In the cubic phase, on the other hand, the micellar rotational diffusion is severely hindered. Moreover, the micelles are no longer spherical, and consequently, the lateral diffusion over the curved surface no longer averages the relevant interaction to zero.[24−26] In the cubic phase, the process that eventually averages the interaction to zero is the exchange between micellar "bound" surfactant and monomeric "free" surfactant in the solution. This exchange is essentially determined by the concentration of free surfactant,[23] which in the present system is quite low (see below), leading to a rather slow exchange and broad lines.

The features of the NMR spectra have consequences for the self-diffusion measurements. Water and Ac^- can be separated as well-defined peaks with fast diffusion. By contrast, the peaks from PA^- overlap with the ones from CTA^+. In the micellar solutions, the similar relaxation rates and chemical shifts of CTA^+ and PA^-, together with the fact that the intensity of the PA^- signal is considerably lower than that of the CTA^+ signal, make it difficult to quantify the PA^- diffusion. The situation in the cubic phase, with the broad resonance line (short T_2) of CTA^+, is different. The difference in relaxation between PA^- and CTA^+ makes it possible to use the PFG SE sequence as a "filter" to isolate the PA^- signal. Hence, diffusion measurements of PA^- are feasible in the cubic phase but not in the micellar solution. For PA^-, the narrow peaks from the heterounits (see Materials and Methods) turned out to be the most favorable signals for diffusion measurements. Independent measurements on a simple NaPA solution showed that the heteronunits diffused at the same rate as the acrylate units, thus confirming that the heterounits were indeed integral parts of the polyacrylate ion.

Polyacrylate Diffusion. One important experimental aspect of polymer diffusion is the polydispersity of the polymer.[27,28] A full description of the polydispersity is given by the molecular weight distribution, $P(M)$. The distribution of molecular weights gives rise to a diffusion coefficient distribution, $P(D)$, through[27,29]

$$P(D)\,\mathrm{d}D = MP(M)\,\mathrm{d}M \tag{6}$$

The different weight fractions of a polydisperse polymer usually have identical chemical shift and relaxation times but different values of D. The echo attenuation for such a system is given by

$$E(k) = \int_0^\infty P(D)\exp(-kD)\,\mathrm{d}D \tag{7}$$

where $P(D)$ is a normalized distribution of diffusion coefficents. A plot of ln E vs k will in general not give a straight line for a polymer. The wider the distribution of D is, the higher the curvature will be.

The extraction of $P(D)$ from experimental $E(k)$ is not trivial, a fact well-known from dynamic light scattering[30] and NMR relaxation.[31] Many distributions satisfy the same set of experimental data, and the choice of distribution is preferably based on information from other sources. However, it has been shown that the *average* value, quantified by the first moment $\langle D\rangle$ of the distribution, is comparatively easily estimated by assuming a form for the distribution that is not necessarily the correct one.[32] The relevant criteria are that the distribution function should have few adjustable parameters and be able to reproduce the data. Accordingly, to describe the PA^- diffusion, we chose a distribution consisting of two discrete components, one fast (f) and one slow (s). The echo attenuation in this case is biexponential

$$E(k) = p_\mathrm{f}\exp(-kD_\mathrm{f}) + (1 - p_\mathrm{f})\exp(-kD_\mathrm{s}) \tag{8}$$

where p_f is the fraction of the fast component. The first moment is given by

$$\langle D\rangle = \int_{-\infty}^{\infty} DP(D)\,\mathrm{d}D = p_\mathrm{f}D_\mathrm{f} + (1 - p_\mathrm{f})D_\mathrm{s} \tag{9}$$

Figure 8a shows that the chosen distribution, eq 8, succeeds quite well in describing the experimental echo attenuations. We emphasize, however, that the success of the fits should not be taken to suggest that the polyion consists of two discrete fractions.

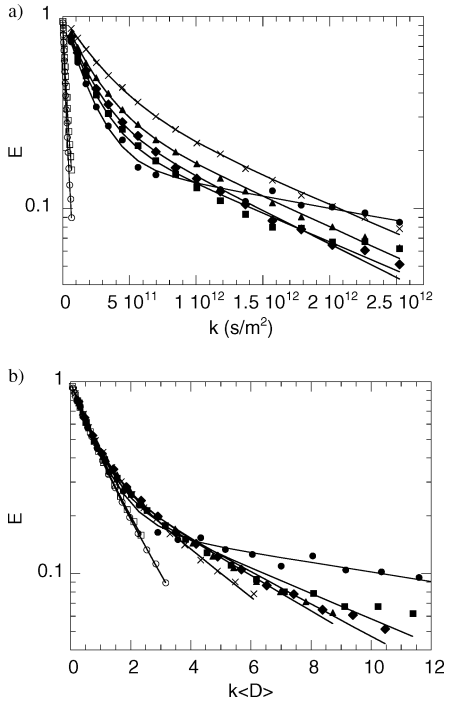

Figure 8. Polyion diffusion in the cubic phase (filled symbols) shown as (a) E vs k and (b) E vs $k\langle D\rangle$ at different ion compositions: x_{Ac} = 0.6 (●), 0.45 (■), 0.3 (◆), 0.2 (▲), and 0 (×). The empty symbols denote the diffusion in a 25 wt % NaPA solution.

A further complication is that the dependence of the diffusion coefficient on the molecular weight is not universal. For instance, for simple polymer solutions, the scaling is

$$D \propto M^{-0.5} \tag{10}$$

in the dilute concentration region, whereas for semidilute and concentrated solutions (above c^*, the overlap concentration), there is a much stronger dependence on the molecular weight[33] given by

$$D \propto M^{-2} \tag{11}$$

The scaling of D with M is most easily visualized by plotting ln E as a function of $k\langle D\rangle$. Figure 8b compares, in such a plot, data for PA^- in simple aqueous NaPA solutions with data for the polyion in cubic samples. The initial slope is the same for all curves, indicating that the evaluation of $\langle D\rangle$ from the assumption of two discrete components is numerically appropriate, although it should not be a correct model of the system. Most interestingly, the data are separated in two groups with markedly different scaling behavior: the NaPA solutions give almost straight lines, whereas the cubic samples show a strong curvature. It is clear that the dependence of the self-diffusion on the molecular weight distribution is strongly amplified in the cubic phase.

Self-Diffusion Results from the Cubic Phase. Figure 9 shows the diffusion coefficients of H_2O, Ac^-, PA^-, and CTA^+ as a function of the fraction of simple counterions, x_{Ac}, in the cubic phase. For the PA^- component, the values shown are the average diffusion coefficients, $\langle D\rangle$, evaluated as described in the previous section. The diffusion coefficients of the four molecular species are dispersed over 4 orders of magnitude, from 10^{-10} to 10^{-14} m^2/s, illustrating the power of the NMR self-diffusion technique. The fastest diffusing molecule in the system is water (measured as HDO), followed by the acetate ion, the polyacrylate ion, and the surfactant. A striking feature

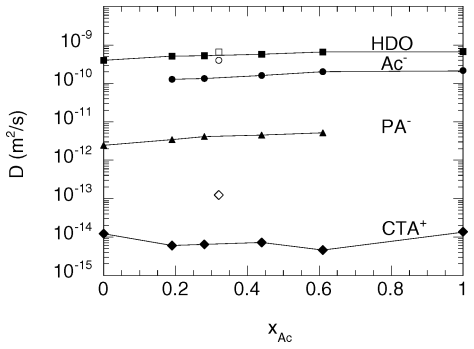

Figure 9. Diffusion coefficients, D, in the cubic phase (filled symbols) as a function of the counterion composition, x_{Ac}, for HDO (■), Ac^- (●), PA^- (▲), and CTA^+ (◆). Empty symbols show the corresponding diffusion coefficients in a micellar sample with a comparable water content (55 wt %) obtained at x_{Ac} = 0.3.

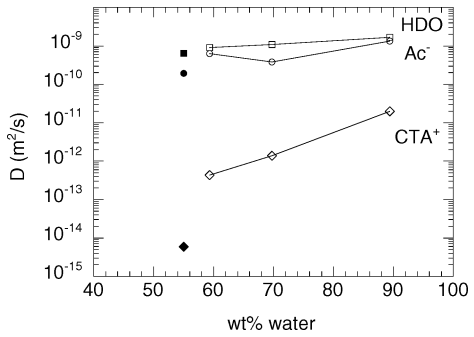

Figure 10. Diffusion coefficients, D, in the micellar phase (empty symbols) as a function of the water content at constant x_{Ac} = 0.7 for HDO (□), Ac^- (○), and CTA^+ (◇). The filled symbols show the corresponding diffusion coefficients in the cubic phase at x_{Ac} = 0.7.

of Figure 9 is the weak variation of all diffusion coefficients with the counterion composition.

The rates of diffusion of H_2O, Ac^-, and PA^- all increase slightly with increasing x_{Ac}. Evidently, the presence of polacrylate ions hinders the diffusion to some extent. The water diffusion coefficient increases from 4.0×10^{-10} m^2/s at x_{Ac} = 0 to 6.7×10^{-10} m^2/s at x_{Ac} = 1. The acetate diffusion coefficient increases from 1.3×10^{-10} m^2/s at x_{Ac} = 0.2 to 2.2×10^{-10} m^2/s at x_{Ac} = 1. The ratio of the two diffusion coefficients, D_{HDO}/D_{Ac}, is larger at low x_{Ac}, indicating that the acetate diffusion is more restricted than the water diffusion by the presence of the polyions. The polyion diffusion coefficient is on the order of 10^{-12} m^2/s.

The diffusion of the CTA^+ ions was difficult to measure owing to the fast transverse relaxation. Hence, the obtained values should be seen as approximate diffusion coefficients. The values obtained are on the order of 10^{-14} m^2/s and do not show any clear trend with the change in counterion composition.

Self-Diffusion Results from the Micellar Phase. As detailed above, it was not possible to measure the PA^- diffusion in the micellar phase. The acetate diffusion was also difficult to follow because of the small amplitude of the acetate peak. On the other hand, the large CTA^+ peaks made it possible to study the diffusion of the surfactant ion without the difficulties of fast relaxation times encountered in the cubic phase. The effect of varying the counterion composition was tested for samples containing 73 wt % water (see Figure 2). As in the cubic phase, this effect was quite small with a weak increase in all diffusion coefficients (HDO, Ac^-, and CTA^+) with increasing x_{Ac}.

As expected, the diffusion rates of all molecules increase when the water content increases. This is shown for x_{Ac}= 0.7 in Figure 10. Included are also data from the cubic phase,

TABLE 2: Diffusion Coefficients in a Dilute Water Solution

molecule	D_0 (m^2/s)
HDO	1.9×10^{-9} [a]
Ac^-	8.5×10^{-10} [b]
PA^-	1.5×10^{-10} [c]
CTA^+	3.6×10^{-10} [d]

[a] From ref 44. [b] Measured in 0.25 M (~2 wt %) NaAc solution.[45] [c] Measured in 1 wt % NaPA solution. [d] See ref 46.

obtained by interpolation to $x_{Ac} = 0.7$ of the data in Figure 9. The diffusion data for water and acetate vary weakly with the water content and follow the same concentration dependences across the phase boundary. This is expected because the diffusion of these small molecules should be insensitive to the crystallization of the micelles. By contrast, the CTA^+ diffusion increases dramatically in the micellar phase, where the diffusion of micelles (rather than the diffusion of free surfactant molecules, as in the cubic phase) is the dominating transport mechanism. A similar large difference in the CTA^+ diffusion is seen if cubic and micellar samples of similar concentrations are compared, compare the data for a single highly concentrated micellar phase included in Figure 9.

Within the micellar phase, the diffusion of CTA^+ varies more strongly with the water content than the diffusion of the small water and acetate molecules, see Figure 10. This is expected because the effective excluded volume, generated by the micelles, is much larger for other micelles than for small molecules. Note that the effective distance of closest approach for a pair of micelles is affected not only by the micellar radius but also by the long-range double-layer repulsion.

Discussion

Interpretation of the Diffusion Data. Table 2 lists the diffusion coefficients in a dilute water solution, D_0, for each of the molecular species of our systems. Clearly (cf., the data in Figures 9 and 10), the molecular diffusion in a concentrated CTAPA/CTAAc/water mixture is generally reduced compared to the situation in free solution. Moreover, the relative extent of the reduction differs for the various diffusing species. Our objective is now to understand the origin of these effects.

A CTAPA/CTAAc/water mixture can be viewed as a system containing positively charged spheres, the CTA^+ micelles, surrounded by a continuous aqueous domain, see Figure 1. A cubic sample contains stationary micelles ordered in a crystal lattice, whereas a micellar sample is a disordered solution of mobile micelles. Each of the solute molecules, CTA^+, Ac^-, and PA^-, can be either free in the aqueous domain or bound to the micelles. Water, being the solvent, can be either free or bound (as hydration water) to any one of the three solutes. There are several factors causing the decrease in diffusion rate in such a system. A binding to the other molecules or to the micellar aggregates obviously affects the diffusion. In addition, the micelles and the large polyion molecules function as obstacles that restrict the number of possible diffusion paths for the diffusing molecules. Below, we will discuss each one of these effects.

The micellar aggregates obstruct the diffusion of all molecules in the aqueous domain because they make the diffusion path more tortuous. This effect is described by the obstruction factor, $1/\alpha$. For a small, free molecule in the aqueous domain, this obstruction is the sole factor responsible for the decrease in the long-range diffusion rate. Accordingly, for such a case, we obtain[34,35]

$$\frac{1}{\alpha} = \frac{D}{D_0} \tag{12}$$

where D is the effective long-range diffusion coefficient for the small molecule, and D_0 is its diffusion coefficient in a dilute aqueous solution.

In the present system, the solvent between the micelles contains not only small molecules but also polyions, which are another hindrance for the diffusing molecules. An effective polyion obstruction factor, f_{PA}, may be estimated experimentally by comparing the diffusion coefficient of a molecule in a concentrated polyion solution (similar in composition to the aqueous domain of the cubic structure) with the diffusion coefficient in a dilute water solution. For a water molecule, f_{PA} also includes possible effects of binding to the polyion.

The diffusion rate in a micellar solution is also affected by "binding" to the micelles. The detailed nature of this binding is different for the different molecules. Most of the surfactant ions are truly bound in the surfactant aggregates. The water molecules may be attached to the micellar surface by hydration. The negatively charged counterions are attracted to the positively charged micellar aggregates by electrostatic forces. In the simplest possible approach, we may treat the effect of each of these attractive interactions by dividing each diffusing species in two fractions, one that is bound to the micelle (and therefore diffuses with the micelle) and one that is freely diffusing in the aqueous domain.

Within this picture, the diffusion coefficient of a diffusing molecule can be written as a population-weighted average of the diffusion coefficients of the free and bound molecules:

$$D = \frac{1}{\alpha} f_{PA}(1 - p_{mic}) D_0 + p_{mic} D_{mic} \tag{13}$$

where p_{mic} is the fraction of molecules bound to the micelles, D_0 is the diffusion in a dilute water solution, and D_{mic} is the long-range diffusion coefficient of the micelles. Only the free molecules are affected by the obstruction factors discussed above. (Of course, the diffusion of the micelles, and all species bound to the micelles, is also influenced by the presence of other micelles and polyions; these effects are, however, incorporated in D_{mic}.)

Consequently, there are four unknown parameters quantifying the reduction in diffusion of a molecule: α, f_{PA}, p_{mic}, and D_{mic}. In the cubic phase, it is reasonable to write $D_{mic} = 0$. With this assumption, the second term in eq 13 vanishes, thus leaving three unknown parameters.

Obstruction by Micelles. The obstruction by the micelles depends both on their concentration and on their shape. Theoretical calculations have been made for pointlike molecules diffusing in dispersions of spherical, prolate, or oblate colloidal particles. Jönsson et al.[36] have used the cell model for such calculations. For spheres, the obstruction factor was given by the expression $(1 + 0.5\phi)^{-1}$, where ϕ is the volume fraction of spheres. A system containing 40 vol % spheres (which roughly corresponds to the volume fraction in the cubic phase) reduces the diffusion coefficient of the solvent molecules by a factor of 0.83. Approximately the same obstruction factor was obtained for prolates, whereas oblates gave a reduction factor of 0.75, in both cases for moderate axial ratios.

Jóhannesson et al.[37] used random-flight simulations to investigate obstructions ordered on primitive and face-centered cubic lattices. The obstruction factor for 40 vol % spheres was 0.8 in a primitive lattice and 0.85 in a face-centered lattice. Also here, the largest obstruction factors were obtained for oblates.

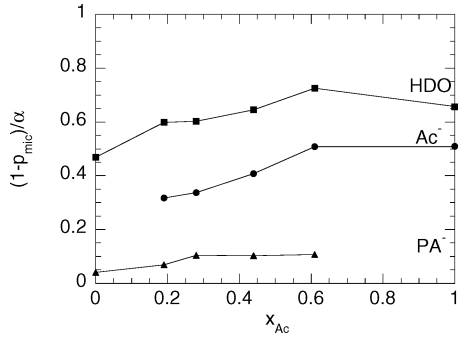

Figure 11. Plot of $(1 - p_{mic})/\alpha$ (see text) in the cubic phase as a function of the counterion composition, x_{Ac}.

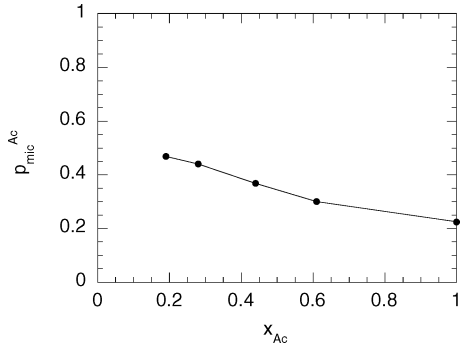

Figure 12. The fraction of bound acetate molecules in the aqueous domain of the cubic structure, p_{mic}^{Ac}, as a function of the counterion composition, x_{Ac}.

Obstruction by Polyions. To estimate the factor f_{PA} in the cubic samples, a series of samples with compositions corresponding to the aqueous domains in the cubic samples were prepared. The measured diffusion coefficients in these NaPA/NaAc/D_2O mixtures give the diffusion coefficients in the absence of micellar obstruction but with the same concentrations of acetate and polyacrylate as in the cubic samples. Thus these measured values should correspond to the product $f_{PA}D_0$, in eq 13.

With $D_{mic} = 0$ in a cubic phase, the ratio $D/(f_{PA}D_0)$ equals $(1 - p_{mic})/\alpha$, according to eq 13. This ratio thus contains contributions from both obstruction and binding. In Figure 11, the factor $(1 - p_{mic})/\alpha$, obtained from the ratio of the measured diffusion coefficients as just described, is plotted versus the ion composition for the various diffusing species in the cubic phase. In the absence of any binding to the micelles and with the same obstruction factor for all three diffusing species, the data for PA^-, Ac^-, and HDO would collapse on a single curve in Figure 11. This is obviously not the case. The highest value of the factor $(1 - p_{mic})/\alpha$ is obtained for water (roughly 0.6), whereas the values for acetate and polyacrylate are ca. 0.4 and 0.1, respectively.

As we saw in the previous section, theoretical estimates of the obstruction factor vary between 0.75 and 0.83, depending on the chosen shape of the particle and the structure of the lattice. The measured factors $(1 - p_{mic})/\alpha$ for water in the cubic phase are not too far below this value. We may thus assume $p_{mic} \approx 0$ for water. The additional retardation of the diffusion of acetate in Figure 11 should then be an effect of binding to the micelle because the obstruction factor may be assumed to be the same for acetate as for water. The latter assumption should be inappropriate for the polyion, as will be discussed in more detail below.

Calculation of Free and Bound Ac^- and CTA^+. If water, Ac^-, and CTA^+ can be regarded as small molecules and the assumption of no bound water molecules is used, we may apply eq 13 to calculate the fraction of bound acetate and CTA^+ molecules. Rearranging eq 13 (using the assumptions that $D_{mic} = 0$ and that the water data in Figure 11 represent the pure obstruction factor at each value of x_{Ac}, as discussed previously), we obtain the fraction of bound acetate molecules, p_{mic}^{Ac}, in the cubic phase as

$$p_{mic}^{Ac} = 1 - \frac{(D/(f_{PA}D_0))_{Ac}}{(D/(f_{PA}D_0))_{HDO}} \qquad (14)$$

Figure 12 shows p_{mic}^{Ac} as a function of the mole fraction of acetate counterions in the cubic phase, x_{Ac}. Approximately 40% of the acetate ions are bound. Similar calculations for the micellar phase, taking into account the finite diffusion coefficient of the micelles, gave a similar fraction of bound acetate ions. The degree of counterion binding obtained here is comparatively low, especially for the pure CTAAc micelles. In general, micelles of ionic surfactants are considered to have 60−70% bound counterions.[38] From NMR self-diffusion measurements, Stilbs and Lindman obtained as much 80% of bound counterions for decylammonium dichloroacetate micelles.[39] The uncertainty in the micellar obstruction factor used in our calculations can account for part, but not all, of this discrepancy. For instance, if we use (instead of the experimental water data from Figure 11) the theoretical obstruction factor 0.83 in the cubic phase, we obtain p_{mic}^{Ac} in the range 0.39−0.62.

We can also calculate the fraction of bound surfactant in the cubic phase. We assume that the free CTA^+ ion is small enough to experience the same obstruction effects as the water molecule in the aqueous domain of the cubic structure. As for acetate, the difference in the diffusion between the molecules would then be due to the fraction of CTA^+ ions bound in the micelles. Because f_{PA} was not determined for CTA^+ ions, we will furthermore assume that f_{PA} is the same for free surfactant ions as for water. The polyion obstruction factors thus cancel in eq 14, and the fraction of free surfactant can be calculated by inserting the experimental ratios D/D_0 for CTA^+ ions and water, respectively. A fraction of free surfactant on the order of 10^{-4} is obtained. The majority of the surfactant ions, >99.99%, are thus bound in the micellar aggregates. The amount of free surfactant corresponds to a concentration of 0.3 mM in the aqueous domain. Considering the cmc of CTAAc, which is 1.6 mM,[40] this number is reasonable. The lowering of the free concentration below the value of cmc is due to electrostatic effects.[39]

Alternatively, one may from the value of the diffusion coefficient and the size of the unit cell estimate the lifetime of a surfactant ion in a micellar aggregate. The lifetime, τ, can be written as

$$\tau = \frac{\langle b^2 \rangle}{6D} \qquad (15)$$

where b is the distance between the center of the aggregates in the cubic phase.[41] The $Pm3n$ unit cell has a compact structure and contains several micellar distances because the micelles are situated in the center, corners, and walls of the cubic unit cell. An approximate distance between the centers of the aggregates can be taken as half the size of the unit cell. The lifetime in a micelle varies in the range 0.3−1 ms for the different samples, showing no systematic dependence on the counterion composition (see Table 3). The long lifetime is consistent with the broad lines of the NMR spectra (see Figure 7).

TABLE 3: The Lifetime of a Surfactant Ion in a Micelle in the Cubic Phase

x_{Ac}	D_{CTA} ($\times 10^{14}$ m^2/s)	interaggregate distance[a] (Å)	τ[b] (ms)
1	1.4	52.1	0.3
0.6	0.5	53.0	1.0
0.45	0.7	52.7	0.6
0.3	0.6	52.8	0.7
0.2	0.6	52.0	0.7
0	1.2	51.7	0.4

[a] Estimated as half of the size of the cubic unit cell, see Table 1. [b] Obtained according to eq 15.

Diffusion of the Polyion. Two features of the polyion diffusion in the cubic samples are notable. First, the polyion diffusion is much more retarded than the diffusion of the small acetate molecule (see Figure 11). Second, the molecular weight dependence of the diffusion coefficient is much stronger in a cubic phase than in a simple polyelectrolyte solution (see Figure 8b). We see two candidate mechanisms that could give rise to these effects. The electrostatic interactions should be stronger for a polyion than for a small ion, and they should also increase in strength with increasing polyion length. In terms of eq 13, electrostatics should give a large value of p_{mic} and a variation in p_{mic} with molecular weight. The other mechanism is a strong obstrucion because the distance between micelles is not much larger than the radius of gyration of the polyion. Again, the extent of the obstruction should vary with the molecular weight of the polyion.

A liquid crystalline phase may be modeled as a network of pores. The diffusion of a particle in a porous medium is strongly dependent on the size of the pores or, more precisely, on the ratio of the size of the particle and that of the pore. According to Sahimi et al.,[14] the diffusion of a particle in a medium made of a network of cylindrical pores can be written as

$$D \propto \exp\left(-\mu \frac{a}{R}\right) \tag{16}$$

where μ is a constant, a is the particle radius (related to the molecular weight M), and R the pore cylinder radius. Sahimi et al. concluded that the particle diffusion is strongly reduced for $a/R > 0.1$. In our case, the "pore cylinder radius" would correspond to the distance between the micellar aggregates in the cubic phase. Taking a distance of 50 Å implies that any polymer chain of a size greater than 5 Å would be affected by the network.

Of course, the ansatz represented by eq 16 is probably too simplistic for the present case. It seems likely that the translation of the polyions in the system studied here may be pictured as an effectively two-dimensional diffusion on the surface of a micelle. The long-range diffusion would then depend on the time scale of the surface diffusion and on the probability for a polyion to diffuse from a given micelle to its neighbor.

Concluding Remarks

This study contains the first measurements of molecular self-diffusion in concentrated mixtures containing a charged surfactant and an oppositely charged polymer. The CTAPA/CTAAc/water system has shown to be quite well suited for such studies. In the ordered cubic phase, in particular, it has been possible to measure the diffusion coefficients of all molecular species over the entire composition range of monovalent/polymeric counterions.

A striking feature of the studied system is the weak dependence of all diffusion coefficients on counterion composition, as long as the comparisons are made at a constant water content within a single-phase region. This confirms the uniformity of the phases. The observed diffusion coefficients of water, monovalent counterions, and surfactant ions may be accounted for in a simple model, considering obstruction effects and, for the surfactant ions and counterions, binding to the micelles. The analysis yields reasonable numbers both for the obstruction effect and for the fractions of surfactant ions and monovalent counterions that are bound to the micelles.

From a more general perspective, an oppositely charged polymer−surfactant system clearly represents an interesting model system for studies of polymer diffusion in porous media. One useful feature of the system is that the polyion is forced to stay inside the structure, owing to the electrostatic interactions. In general, it is difficult to trap a polymer solution in a confined space because the polymer component is strongly excluded for entropic reasons. Thus, mixtures of nonionic polymers with nonionic surfactant micelles typically display a segregative phase separation at high concentrations, resulting in a concentrated micellar phase, virtually free of polymers, in equilibrium with a semidilute polymer solution.[42] In an oppositely charged system it is, furthermore, possible to modulate the strength of the attractive polyion−micelle interaction simply by adding salt, which increases the versatility of the system. Studies by Thalberg et al. have shown that it is possible to cover the entire range from an associative to a segregative phase separation by adding salt.[43]

The polyion diffusion observed in this work displays some interesting features. The polyions in the cubic phase are quite mobile, but they are nevertheless retarded by a factor of 10 compared to their diffusion in a simple polyelectrolyte solution containing the same weight ratio of polyion to water. As an alternative comparison, the relative retardation is a factor 4 stronger for the polyions than for the monovalent counterions. Moreover, there is a strongly enhanced molecular weight dependence of the polyion diffusion in the cubic phase. A molecular understanding of the polyion diffusion, and the molecular weight dependence in particular, requires further investigation.

Acknowledgment. Bernard Cabane, ESPCI, Paris, is acknowledged for performing X-ray measurements at L.U.R.E. The project was funded by the Swedish National Graduate School of Colloid and Interface Technology (A.S. and D.T.) and the Swedish Research Council (L.P. and O.S.).

References and Notes

(1) Goddard, E. D.; Anathapadmanabhan, K. P. *Interactions of surfactants with polymers and proteins*; CRC Press: Boca Raton,FL, 1993.

(2) Kwak, J. C. T. *Polymer-surfactant systems*; Marcel Dekker: New York, 1998.

(3) Thalberg, K.; Lindman, B. Polymer-surfactant interactions—recent developments. In *Interactions of surfactants with polymers and proteins*; Goddard, E. D., Ananthapadmanabhan, K. P., Eds.; CRC Press: Boca Raton, FL, 1993; p 203.

(4) Piculell, L.; Lindman, B. *Adv. Colloid Interface Sci.* **1992**, *41*, 149.

(5) Ilekti, P.; Piculell, L.; Tournilhac, F.; Cabane, B. *J. Phys. Chem. B* **1998**, *102*, 344.

(6) Antonietti, M.; Conrad, J. *Angew. Chem., Int. Ed. Engl.* **1994**, *33*, 1869.

(7) Claesson, P. M.; Bergström, M.; Dedenaite, A.; Kjellin, M.; Legrand, J.-F.; Grillo, I. *J. Phys. Chem. B* **2000**, *104*, 11689.

(8) Ilekti, P.; Martin, T.; Cabane, B.; Piculell, L. *J. Phys. Chem. B* **1999**, *103*, 9831.

(9) Kogej, K.; Evmeneko, G.; Theunissen, E.; Berghmans, H.; Reynaers, H. *Langmuir* **2001**, *17*, 3175.

(10) Merta, J.; Torkkeli, M.; Ikonen, T.; Serimaa, R.; Steniua, P. *Macromolecules* **2001**, *34*, 2937.
(11) Zhou, S.; Chou, B. *Adv. Mater.* **2000**, *12*, 545.
(12) Svensson, A.; Piculell, L.; Cabane, B.; Ilekti, P. *J. Phys. Chem. B* **2002**, *106*, 1013.
(13) Svensson, A.; Piculell, L.; Karlsson, L.; Cabane, B.; Jönsson, B. *J. Phys. Chem. B* **2003**, *107*, 8119.
(14) Sahimi, M.; Jue, V. L. *Phys. Rev. Lett.* **1989**, *62*, 629.
(15) Söderman, O.; Stilbs, P. *Prog. Nucl. Magn. Reson. Spectrosc.* **1994**, *26*, 445.
(16) Nydén, M.; Söderman, O. *Langmuir* **1995**, *11*, 1537.
(17) Morrison, R. T.; Boyd, R. N. *Organic Chemistry*, fourth ed.; Allyn and Bacon Inc.: Newton, MA, 1983.
(18) Callaghan, P. T. *Principles of nuclear magnetic resonance microscopy*, 1st ed.; Oxford University Press: Oxford, U.K., 1991.
(19) Kimmich, R. *NMR: tomography, diffusometry, relaxometry*, 1st ed.; Springer-Verlag: Berlin, 1997.
(20) Fontell, K. *Colloid Polym. Sci.* **1990**, *268*, 264.
(21) Evans, D. F.; Wennerström, H. *The colloidal domain − where physics, chemistry, biology and technology meet*, 2nd ed.; John Wiley & sons: New York, 1999.
(22) Johansson, L. B.-Å.; Söderman, O. *J. Phys. Chem.* **1987**, *91*, 5275.
(23) Söderman, O.; Johansson, L. B. A. *J. Colloid Interface Sci.* **1996**, *179*, 570.
(24) Halle, B. *Mol. Phys.* **1987**, *61*, 963.
(25) Halle, B. *J. Chem. Phys.* **1991**, *94*, 3150.
(26) Halle, B. *Liq. Cryst.* **1992**, *12*, 625.
(27) Callaghan, P. T.; Lelievre, J. *Biopolymers* **1985**, *24*, 411.
(28) Nydén, M.; Söderman, O. *Macromolecules* **1998**, *31*, 4990.
(29) Håkansson, B.; Nydén, M.; Söderman, O. *Colloid Polym. Sci.* **2000**, *278*, 399.
(30) Jakes, J. *Collect. Czech. Chem. Commun.* **1995**, *60*, 1781.
(31) Overloop, K.; Van Gerven, L. *J. Magn. Reson.* **1992**, *100*, 303.
(32) Topgaard, D.; Söderman, O. *J. Phys. Chem. B* **2002**, *106*, 11887.
(33) Fleischer, G. *Polymer* **1985**, *26*, 1677.
(34) Bear, J. *Dynamics of fluids in porous media*; Dover Publications: New York, 1988.
(35) Latour, L. L.; Kleinberg, R. L.; Mitra, P. P.; Sotak, C. H. *J. Magn. Reson. A* **1995**, *112*, 83.
(36) Jönsson, B.; Wennerström, H.; Nilsson, P.-G.; Linse, P. *Colloid Polym. Sci.* **1986**, *264*, 77.
(37) Jóhannesson, H.; Halle, B. *J. Chem. Phys.* **1996**, *17*, 6807.
(38) Lindman, B.; Wennerström, H. *Top. Curr. Chem.* **1980**, *87*, 1.
(39) Stilbs, P.; Lindman, B. *J. Phys. Chem.* **1981**, *85*, 2587.
(40) Lynch, I. Unpublished result.
(41) Håkansson, B.; Hansson, P.; Regev, O.; Söderman, O. *Langmuir* **1998**, *14*, 5730.
(42) Piculell, L.; Bergfeldt, K.; Gerdes, S. *J. Phys. Chem.* **1996**, *100*, 3675.
(43) Thalberg, K.; Lindman, B.; Karlström, G. *J. Phys. Chem.* **1991**, *95*, 6004.
(44) Mills, R. *J. Phys. Chem.* **1973**, *77*, 685.
(45) Malmborg, C.; Topgaard, D.; Söderman, O. *J. Colloid Interface Sci.* **2003**, *263*, 270.
(46) Söderman, O. Unpublished result.